NANOMECHANICAL ANALYSIS OF ENZYME-SUBSTRATE COMPLEXES

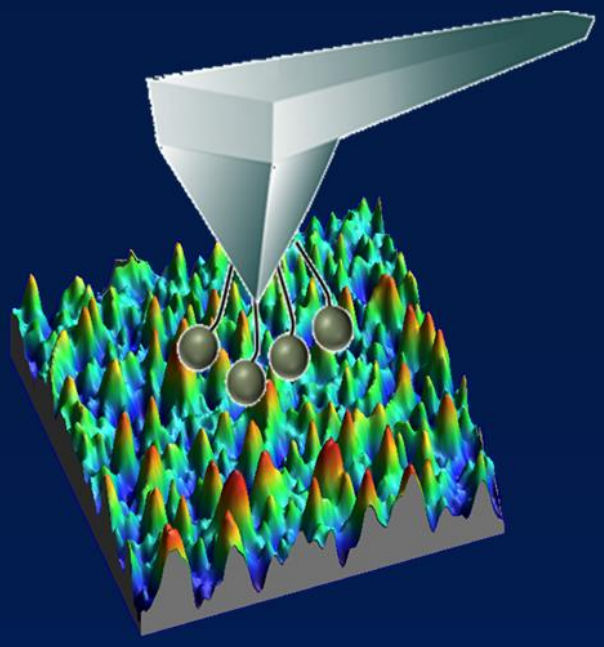

Author: **Silvia Caballero Mancebo**

Advisor: Dr. Anabel Gracia Lostao

Master's Degree in Nanostructured Materials for Nanotechnology Applications.

University of Zaragoza

Universidad
Zaragoza

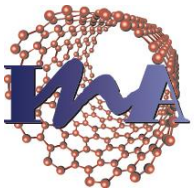

Instituto Universitario de Investigación
en Nanociencia de Aragón
Universidad Zaragoza

LMA
LABORATORIO
DE MICROSCOPIAS
AVANZADAS

Acknowledgements

A number of people deserve thanks for their support and help during this Master thesis. It is therefore my greatest pleasure to express my gratitude to them all.

Foremost, I would like to express my sincere gratitude to my advisor Dr. Anabel Gracia Lostao for her support, her patience, motivation and her insight that lead to the original proposal of studying for the first time the nanomechanical properties of an enzyme-substrate complex.

I wish to thank Dr. Marta Martínez Júlvez (at the Department of Biochemistry and Cellular and Molecular Biology) for the laboratory materials she provided me with. My appreciation also goes out to José Luis Díaz for his time, assistance and good advices dealing with the AFM. I would also like to extend my gratitude to the whole Faculty of this Master, especially to the Master Coordinator, Dr. Pilar Cea whose dedication and hard work has certainly helped us along the way. She always took time out from her busy schedule to give a helping hand both academically and personally.

I would like to thank Cátedra SAMCA for granting the SAMCA Nanotechnology Scholarship to join this program.

Thanks to my fellow lab mates. Carlos, thank you so much for introducing me to the exciting world of force spectroscopy and for guiding me during my first steps with the AFM. Without your unparalleled support, this work would not have gone ahead. Mari Carmen, thank you for your optimism and contagious joy, for your uncontrollable desire to help and for those hours of company (you can't imagine how sorry I am for missing that day, congratulations!). And finally Miren, thank you for your desire to learn, for your hard questions, and above all, for your great help this summer. Good luck in Barcelona!

My special "thanks" (you know how!, no pun intended) to my classmates. I won't forget the endless lab demos, last minute reviews and our after lunch talks. Thank you for listening to me cheering me up when I needed it. I expect visits!!

A special mentioned is due for my friends. You have forgiven my absences, born my burdens and supported me in everything. Paula, it has been great meeting you and living with you. Without you, this year could have been unbearable.

Last but not least, I owe more than thanks to my parents and sister. There is so much for me to thank them that I do not know where to start. They have always supported me, no matter what and have been pivotal in all my successes. Elena, although distance is going to be a hard thing to overcome, I know I will always count on you. Best of luck and reach for the stars. You deserve this and more!

Table of contents

Abbreviations

Abs	Absorbance
AFM	Atomic Force Microscopy
APTES	(3-Aminopropyl)triethoxysilane
C	Concentration
cyt *c*	Cytochrom *c*
Da	Dalton
DFS	Dynamic Force Spectroscopy
DNA	Desoxyrribonucleic acid
DTT	Dithiothreitol
EDTA	Ethylenediaminetetraacetic acid
ET	Electron transfer
F	Applied force
F*	Most probable unbinding force
FAD	Flavin adenine dinucleotide (oxidised)
FADH	Flavin adenine dinucleotide (reduced)
Fd	Ferredoxin
Fld	Flavodoxin
FMN	Flavin mononucleotide
FNR	Ferredoxin-$NAPD^+$ mnReductase
Fz	Force-distance curves
k_B	Boltzmann's constant

k_{cat}	see TON
k_{off}	Dissociation rate constant at zero applied force
l	Path length
$NADP^+$	Nicotinamide adenine dinucleotide phosphate (oxidised)
NADPH	Nicotinamide adenine dinucleotide phosphate (reduced)
NHS	N-hydroxysuccinimide
PDB	Protein Data Bank
PBS	Phosphate Saline Buffer
PEG	Poly(ethylene glycol)
R	Loading rate
rpm	Revolutions per minute
SDS	Sodium dodecyl sulfate
SMFS	Single Molecule Force Spectroscopy
SNOM	Scanning Near Field Optical Microscopy
SPM	Scanning Probe Microscopy
STM	Scanning Tunnelling Microscopy
Sulfo-LC-SPDP	sulfosuccinimidyl 6-[3'(2-pyridyldithio)-propionamido] hexanoate
T	Temperature
τ	Lifetime
TON	Turnover number
wt	wild type
ε	Attenuation coefficient

Abstract

The aim of this thesis is to study for the first time the interaction forces between an enzyme and its enzymatic substrate using a single molecule approach, Atomic Force Spectroscopy (AFS). The enzyme chosen is the Ferredoxin-$NADP^+$ reductase (FNR) involved in the photosynthetic chain accepting electrons from flavoproteins ferredoxin (Fd)/ flavodoxin (Fld) and transfering them to its substrate, $NADP^+$ which is then reduced to NADPH.

To that matter, the enzyme FNR was immobilized on the surface of flat mica pieces and its substrate, $NADP^+$, was immobilize on the surface of prefunctionalized AFM tips carrying a maleimide-PEG linker. The effect that the immobilization process had on the structure and activity of FNR was tested by AFM imaging and enzymatic assays, respectively, showing only a slight decrease on the catalytic activity of the enzyme.

Both the functionalized tip and sample were subsequently used for the AFS measurements. These experiments gave data consisting of hundreds of Fz curves at different loading rates that were used to construct histograms that provided the values for the most probable unbinding force at each different loading rate. 136 pN was obtained as the most probable unbinding force at a loading rate of 10 nN/s.

The unbinding data was analysed in the framework of the Bell-Evans model in order to obtain mechanostability parameters associated with the transition state of the dissociation process. The results showed a single regime, associated to a one-step dissociation kinetic for the FNR:$NADP^+$ complex. The dissociation rate constant, k_{off}, and the x_β (width of the energy barrier) gave 0.0198 s^{-1} and 0.0205 nm, respectively.

These values were indicative of the mechanical stability of the FNR:$NADP^+$ complex, higher than that of FNR with either one of its protein partners. This, together with the lifetime value of the complex, 50.6 s, corroborated our expectations of a strong specificity of FNR for $NADP^+$.

1. INTRODUCTION

1.1. Atomic Force Microscopy

The Atomic Force Microscope (AFM) belongs to a large family of instruments called Scanning Probe Microscopes (SPM) which includes the Scanning Tunnelling Microscope (STM) and the Scanning Near-Field Optical Microscope (SNOM), amongst others (Fig. 1) (Bowen and Hilal, 2009). The basis of all SPM techniques is the use of a very sharp probe to scan a sample of interest. The interaction between the probe and the sample is recorded and used to obtain a high resolution three-dimensional image of the sample surface. The type of image that is built up depends on the type of interaction measured by the probe. The main advantage of SPMs is that, depending upon the technique, they allow the production of images up to the sub-nanometre scale. These images provide quantitative information about the topology and other properties of the sample.

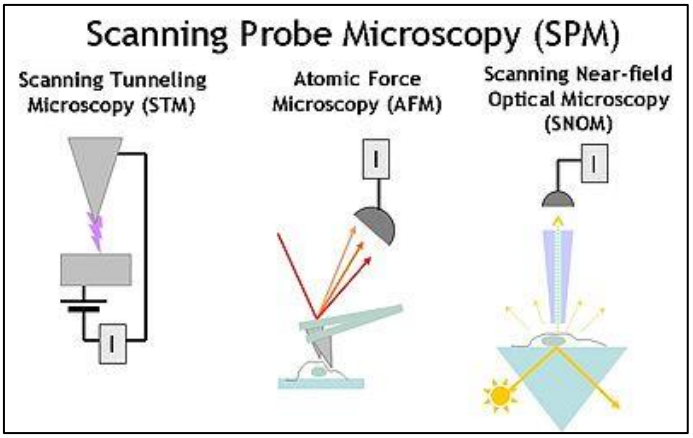

Fig. 1. Scheme showing the basis of several SPMs.

AFM was first described by Binning *et al.*, 1986 as a new method for measuring ultra-small forces on particles as small as a single atom. But what really sets AFM apart from other SPM techniques is the fact that it allows to image the surface of insulators (rather than just magnetic or conductive samples) and biological samples due to its versatility in taking measurements both in air and liquid environments rather than just in high vacuum. Consequently, AFM has been used in a variety of molecular recognition studies involving biological systems under relevant buffer conditions (Bowen and Hilal, 2009).

Molecular recognition studies provide information about specific receptor-ligand interaction forces at the single molecule level and allow to estimate several parameters that characterize that

interaction: mechanical stability, rate dissociation constants, structural data of the binding pocket and the dissociation energy landscape (Bell, 1978; Evans and Ritchie, 1997). Previous studies of these types of interactions using AFM include biotin-avidin (Lee, Kidwell *et al.*, 1994; Floring *et al.*, 1994), antibody-antigen (Hinterdorfer *et al.*, 1996, 1998), sense-antisense DNA (Lee, Chrisey *et al.*, 1994), etc. However, up to our knowledge, there is no publication in which this approach was used to study the interaction between an enzyme and its enzymatic substrate (a non-protein partner) so this project represents a great progress in the field of molecular recognition studies by means of Single Molecule Force Spectroscopy (SMFS) experiments.

1.1.1. Basic principles of AFM

The basic set-up of a typical AFM is shown in Figure 2. In a standard AFM, samples are mounted on a piezoelectric scanner with three-dimensional movement that allows to move the sample in relation to the probe with sub-nanometre accuracy in the three dimensions.

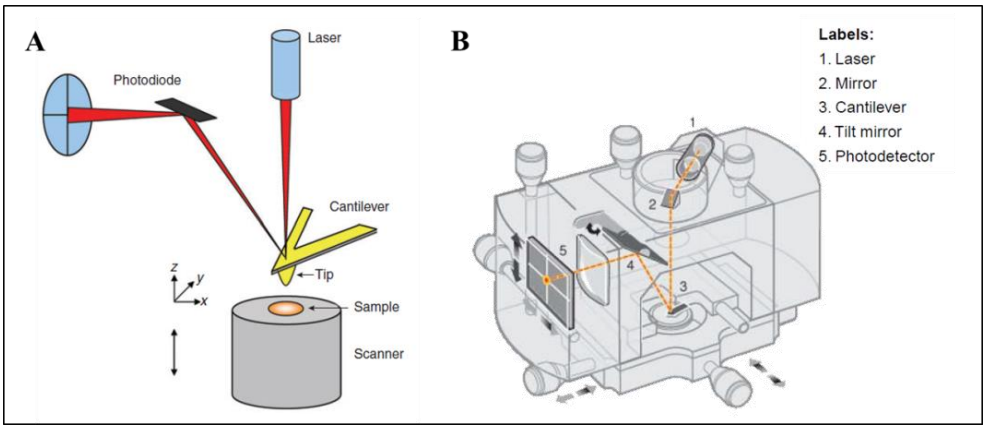

Fig. 2. (A) Standard AFM set-up (Hinterdorfer and Dufrêne, 2006). (B) Holder configuration of the AFM used in this project, a MultiMode 8 AFM (Bruker Digital Instruments, Santa Barbara, USA).

An AFM probe consists of a sharp tip mounted on the end of a flexible cantilever that behaves as a linear or "Hookean" spring. This means that the cantilever deflection can be used to calculate the force which is exerted on the cantilever using Hooke's law (Bowen and Hilal, 2009):

$$F = -k \cdot \Delta x \qquad \text{(Eq. 1)}$$

where F is the force, Δx the deflection of the cantilever and k the spring constant of the cantilever which represents its stiffness.

The probe is brought into and out of contact with the sample surface using a piezoelectric scanner. Movement in this direction is conventionally called the z-axis. The repulsive or attractive forces cause respectively a deflection or a bending of the cantilever which is optically measured by a laser beam reflected in the upper side of the end of the cantilever. Any change in the deflection of the cantilever will produce a change in the position of the laser spot on a quadrupole photodiode. Then the signal in the photodiode is converted into an electric one and used to build the final image (Hinterdorfer and Dufrêne, 2006).

1.1.2. AFM operating modes

As mentioned above, AFM is used to obtain three-dimensional images of surfaces by monitoring the force between the sample and the probe. It is of crucial importance to know the nature of these forces in order to understand how an AFM works (Fig. 3A).

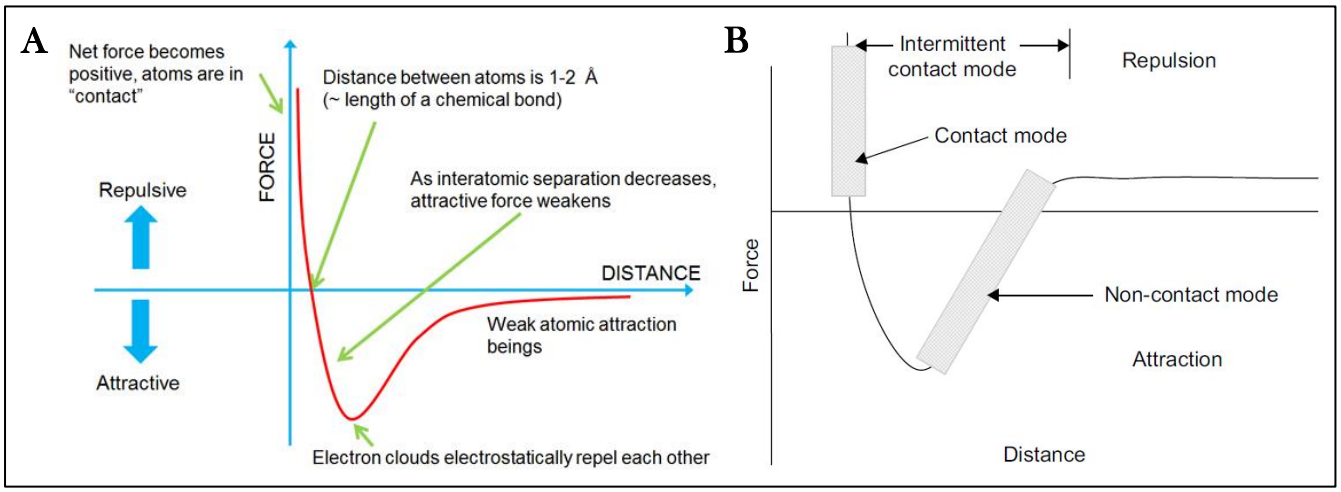

Fig. 3. (A) Force regimes involved in an AFM experiment. (B) Diagram illustrating the force regimes under which each of the three AFM imaging modes operate

Several types of forces are involved in small distances: Van der Waals forces, electrostatic forces, hydrogen bonds…, being the former the main ones. When the AFM tip and the sample surface, that are initially apart, are brought closer together, weak attractive interactions appear between atoms at the surface of the sample and those at the apex of the probe. As the separation distance between tip and sample decreases, the attractive forces increase until electron clouds of both objects begin to interact and electrostatically repel each other. This repulsive force decreases the overall attraction until a net force of zero is reached. Eventually atoms will come into contact so the interaction forces will become positive (repulsive). In this region, the slope of the curve is steep showing that the Van der Waals forces avoid atoms getting closer together. In the case of AFM,

when the cantilever pushes the tip against the sample, the cantilever deflects like a linear spring (Section 1.1.1) (Bowen and Hilal, 2009).

AFM is generally operated using one of the three main feedback modes:

- Contact mode.
- Intermittent contact mode.
- Non-contact mode.

In Figure 3B the different AFM modes are shown as they correspond to the different force regimes explained before.

- **Contact mode:** the tip scans the sample without withdrawing from the surface. In this mode, repulsive Van der Waals forces between the tip and the sample appear. In this mode, the feedback loop of the AFM keeps the force between the tip and the sample constant using the cantilever deflection as signal (Cappella and Dietler, 1999).
  This mode is not suitable for biological samples due to their soft nature and the fact that usually these samples are electrostatically bond to the surface so they can be harmed easily.

- **Intermittent contact mode:** in this case the cantilever is oscillated at its resonant frequency. This is usually done by another piezocrystal placed on the cantilever. Depending on the parameter used as set point for the feedback loop, two different dynamic modes can be distinguished: f*requency-modulation mode (FM-AFM)* and a*mplitude-modulation mode (AM-AFM).* The latter is known as "tapping mode" and is mostly used for liquid measurements of biological samples due to the fact that the tip touches intermittently the sample so damages here are reduced (Zhong *et al.*, 1993).

- **Non-contact mode:** in this mode tip and sample are further separated than in other modes (10 to 100 Å) so that the tip never touches the sample surface so longer range forces are detected. There are two parameters that can be used as set point for the feedback loop, either the force or the height of the tip with respect to the sample (Giessibl, 2003). This mode was developed to precisely image biological samples with no damage to the sample whatsoever.

1.2. Atomic Force Spectroscopy (AFS)

Protein interactions are governed by intermolecular forces and binding energies so their detailed knowledge is pivotal for understanding the nature of their association (Bizzarri and Cannistraro, 2009).

In order to quantitatively describe a biorecognition process, a kinetic analysis is required. In general, biomolecular interactions can be described by the law of mass action. The formation of a complex between two partners, A and B, at equilibrium, can be represented as:

$$A + B \leftrightarrow AB$$

and this association satisfies the following time-dependent equation:

$$d\,[AB]/dt = k_{on}[A][B] - k_{off}[AB] \quad \text{(Eq. 2)}$$

where square brackets stand for the concentration of the molecular species, k_{on} and k_{off} are the association and dissociation rates of the complex, respectively, which describe the kinetics of the interaction. k_{on} is related to the diffusive properties of the biomolecules and depends on the distance and orientation between the partners. However, k_{off} is related to the lifetime, τ_o, of the complex $\left(\tau_o = {k_{off}}^{-1}\right)$ so it provides information about the specificity of the reaction. Moreover, the dissociation rate constant depends on the activation free energy ΔG^* of the reaction (Fig. 4) through:

$$k_{off} = A \cdot e^{(-\Delta G^*/k_B T)} \quad \text{(Eq. 3)}$$

where *A* is the Arrhenius constant, k_B is the Boltzmann constant, and *T* is the absolute temperature (Bizzarri and Cannistraro, 2010).

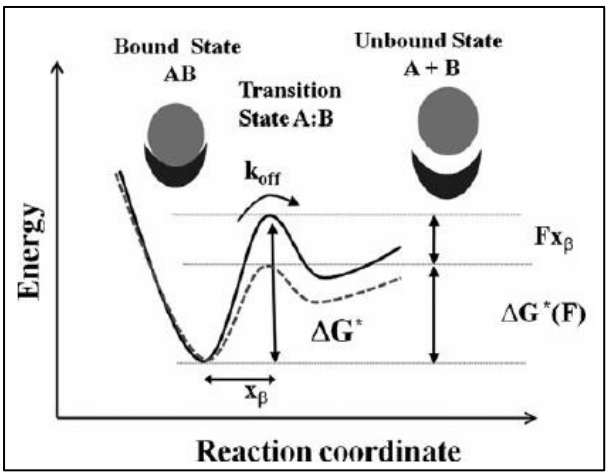

Fig. 4. Schematic diagram of the energy profile for a dissociation process of a biomolecular complex without an external force applied (continuous line) and under the application of an external force, *F*, (dashed line).

This dissociation rate can be determined by various methods. Classical biochemical and biophysical methods only provide a description in bulk. This means that their results are an average of numerous molecules observed at the same time so some aspects, such as transient phenomena, conformation changes, crowding effects, etc., cannot be elucidated since they are hidden in the ensemble average. The strength of AFS is its ability to measure samples at a single molecule level, so that the outcome of each single interaction is recorded. This allows for detailed characterization of the energy landscape of a complex dissociation, which is useful to understand the features of a certain interaction, such as the number, height and the shape of energy barriers, the energy landscape and the rate of the related transitions (Bizzarri and Cannistraro, 2009).

1.2.1. Force-distance curves

In order to measure the unbinding force in a pair of interacting biomolecules by AFS, the functionalized tip carrying one of the interacting partners is approached, at a constant speed, towards the substrate surface onto which the other partner is immobilized. Then, the tip is retracted back to the original position. As the recognition event is a stochastic process, hundreds of these curves are needed in order to obtain statistically relevant data (Noy, 2011). Figure 5 shows an example of a force-distance cycle. Upon approach of the cantilever towards the surface of the sample (dashed line), the attracting forces acting on the tip bend the cantilever. At a certain point (point B) close to the surface, the tip "jumps" towards the surface of the sample (snap into contact). It is now when the ligand on the tip and the receptor on the surface are in physical contact. If the tip is further moved towards the surface, the bending of the cantilever increases linearly because its spring constant is higher than the elasticity of the sample. The approaching phase is stopped (point C) upon reaching a preset maximum value of the contact force (F_c). When the tip is retraced from the surface, it stays in contact with the surface because it is strongly attached as a consequence of the adhesive forces. A force equal to the adhesive force (*unbinding force*) is needed to pull the tip apart from the sample surface (jump out of contact, points E-F). The hysteresis in this type of curves appears as a consequence of this jump-out position being further from the surface than the snap-in one (Bizzarri and Cannistraro, 2012).

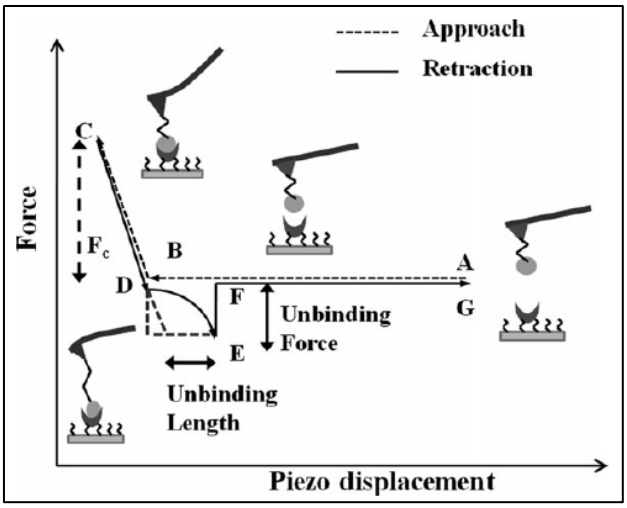

Fig. 5. Diagram of a typical force-distance curve showing a specific unbinding event (Bizzarri and Cannistraro, 2010).

1.2.2. Theoretical models to analyse AFS data

The most common approach used to describe the behaviour of force-induced transformations is based on the seminal works of Bell. Bell's model was proposed for the analysis of cell-cell adhesion bonds and provides a phenomenological description of the effect that mechanical forces have on molecular interactions (Bell, 1978). The main idea is that a forced dissociation can be described as a thermally activated escape over a transition-state barrier and treated within the frame work of the reaction rate theory. At equilibrium, a pair of interacting molecules changes from the bound (AB) to the unbound (A+B) state proceeding over a single transition state (A:B) with a certain activation energy barrier (ΔG^*) (Fig. 5). When an external force is applied, the energy profile of the unbinding process changes by lowering the activation energy of the transition state by $F \cdot x_\beta$ (where F is the applied force and x_β the width of the energy barrier). Now, the dissociation rate constant depends on the applied force, F, as follows (Bizzarri and Cannistraro, 2009):

$$k_{off}(F) = k_{off} \cdot e^{(F \cdot x_\beta / k_B \cdot T)} \quad \text{(Eq.4)}$$

where k_{off} is the dissociation rate at the equilibrium, at zero applied force, with $k_{off} = k_{off}(0)$.

Evans and Ritchie, starting from this assumption, derived a description of the unbinding process in terms of a crossing over a single, sharp barrier through the application of a time-dependent force, $F(t)$. In consequence, this model provides the dependence of the unbinding force on the loading rate, $R = dF/dt$, at which the external force is applied. R is usually given by the

product between the tip retraction speed and the spring constant of the cantilever (Bizzarri and Cannistraro, 2010).

The Bell-Evans model is based on the following assumptions:

- The loading rate during a measurement is constant.
- The unbinding process of a single ligand-receptor pair occurs.
- The rupture time is longer than the diffusional relaxation time, and any rebinding process is neglected.
- The pulling coordinate coincides with the reaction coordinate.
- The width of the energy barrier, x_β, is independent of the applied force.

On this basis, the most probable unbinding force, F^*, can be obtained by calculating the maximum of a probability distribution of the unbinding force as follows (Evans and Ritchie, 1997):

$$F^* = \left(\frac{k_B T}{x_\beta}\right) * ln\left(\frac{R x_\beta}{k_{off} k_B T}\right) \quad \text{(Eq.5)}$$

F^* being the most probable unbinding force, k_B is the Boltzmann constant, T the temperature at which the experiment has been conducted, R the loading rate and k_{off} and x_β the parameters that characterize the complex dissociation, in the case of this project, the FNR:$NADP^+$ enzymatic system (see section 1.2).

The former expression predicts a linear relationship between the most probable unbinding force, F^*, and the natural logarithm of the loading rate, R. By plotting F^* as a function of lnR, the equilibrium parameters k_{off} and x_β can be extracted from the intercept and the slope of the fitting linear curve, respectively (Fig. 6A). In some cases this function exhibits two or more distinct linear regimes (Fig. 6B). Then, two different sets of k_{off} and x_β values can be extracted by two independent linear fits. Such behaviour may be traced back to the presence of two intermediate states in the unbinding process (Bizzarri and Cannistraro, 2009).

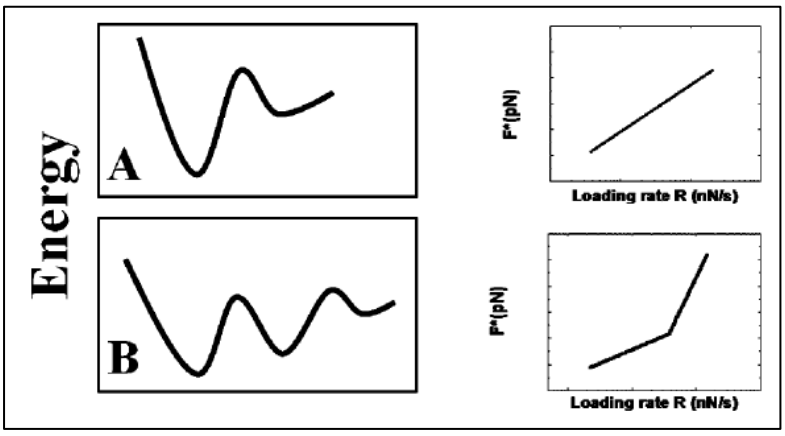

Fig. 6. (Left) Scheme of the energy profile for a dissociation process of a biomolecular complex. (Right) Corresponding trend for the most probable unbinding force as a function of the loading rate.

1.3. Immobilization strategies

The detection of unconstrained ligand-receptor recognition requires a specific linker design (Hinterdorfer *et al.*, 1998). This is one of the most time-consuming steps in an AFM experiment in which the receptor has to be immobilized on a nanometrically flat surface and its ligand has to be attached to the AFM tip.

Generally speaking, there are two main approaches for immobilization of molecules to both the substrate and the tip: either electrostatically or covalently. The main difference between them is the type of established bond. Covalently coupling of both receptor and ligand guarantees that they are sufficiently tight attached as covalent bonds are around 10 times stronger than typical receptor-ligand bonds (Hinterdorfer and Dufrêne, 2006). Loose receptor or ligand fixation may lead to their pull-off from the surface or tip respectively upon the recognition event, resulting in the blocking of the receptor-ligand recognition.

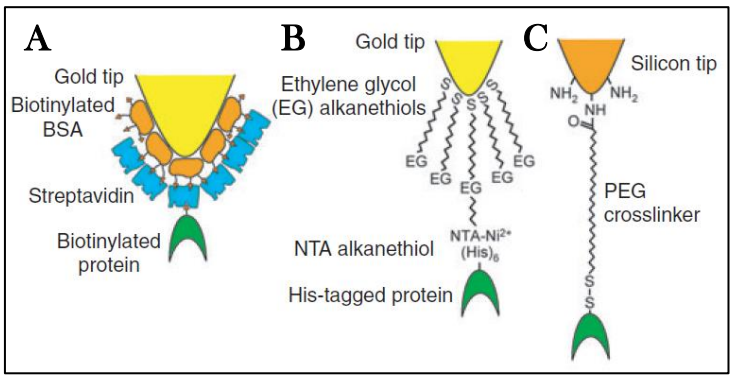

Fig. 7. Different immobilization strategies on AFM tips.

Moreover, the ligand has to be provided with enough motional freedom around the tip so that the recognition process is not influenced by steric restrictions (Bizzarri and Cannistraro, 2012). This is done by using a spacer between the tip and the ligand. Poly(ethylene glycol) (PEG) (Fig. 7C) is used most of the times as crosslinker. It is a water-soluble, nontoxic and non-adhesive flexible polymer.

On the one hand, PEG spacers facilitate the encounters thank to an increase of the motional freedom of the ligand. On the other hand, the use of PEG as spacer also solves one of the main drawbacks of force spectroscopy experiments: providing a fingerprint for identifying the specific events corresponding to the rupture of events. When the receptor on the surface of the sample binds to a ligand on the tip, an attractive force develops upon withdrawing of the tip from the sample

(retrace line in Fig. 5) and increases with tip-sample separation. The same happens when a non-specific interaction between the cantilever and the sample occurs. It is the shape of the curve that determines whether that peak corresponds to a specific interaction or not: the shape of curve in a specific event is determined by the elastic properties of the flexible PEG linker that shows a non-linear, parabolic-like profile that reflects the increment of the spring constant of the linker during extension. Therefore, specific receptor-ligand recognition events are easily distinguishable from linearly shaped non-specific tip-sample adhesion events (Fig. 8) (Hinterdorfer *et al.*, 2000).

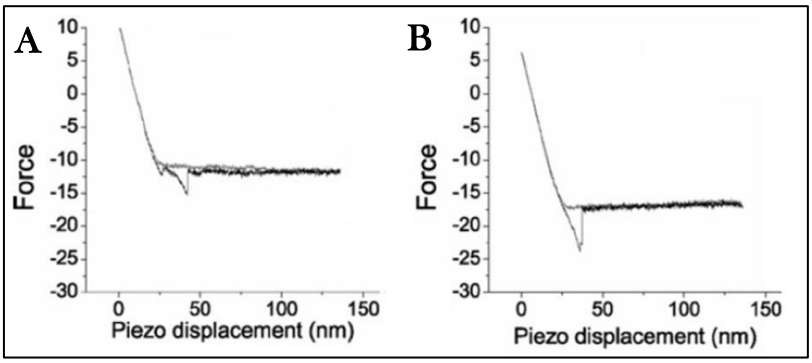

Fig. 8. Real AFS force curves. (A) Specific unbinding event due to the parabolic profile of the peak. (B) Non-specific event since the linear slope of the retrace extends beyond the contact point.

1.4. Ferrodoxin NADP$^+$ reductase

In this project, the system under study is the enzyme Ferredoxin NADP$^+$ reductase (FNR). FNR is a 36 kDa protein (PBD code: 1QUE) that can be found in plants, bacteria and some algae. The FNR used in this project belongs to the cyanobacteria *Anabaena* PCC 7119 and plays a crucial role during the electron transfer (ET) in photosynthesis as the last component of the Photosystem I (PSI) (Fig. 9).

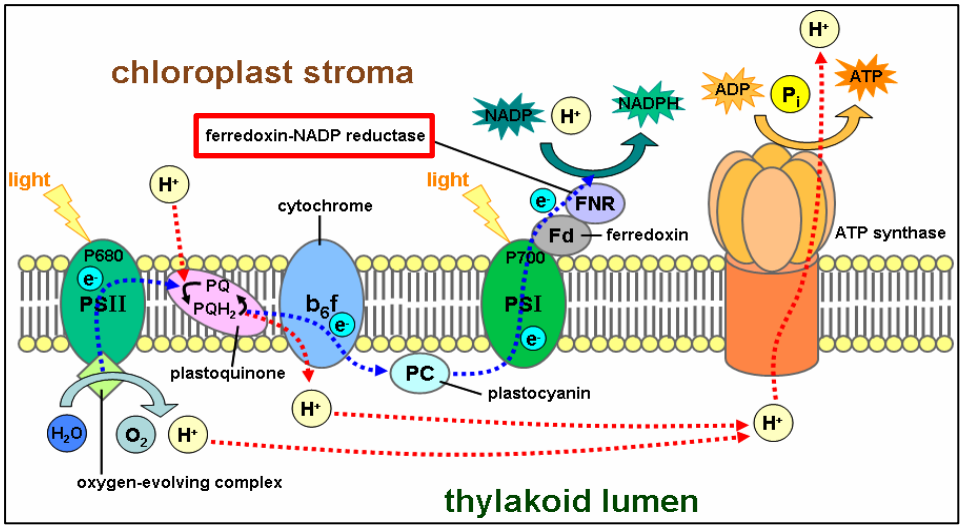

Fig. 9. Scheme of the light reactions during photosynthesis.

It catalyses the sequential transfer of two electrons from two different Ferredoxins (Fd) molecules to a molecule of $NADP^+$ (nicotinamide adenine dinucleotide phosphate) in order to reduce it to NADPH (Fig. 10A) (Jelesarov and Bosshard, 1994). NADPH will then contribute to the Calvin Cycle as a major source of reducing power.

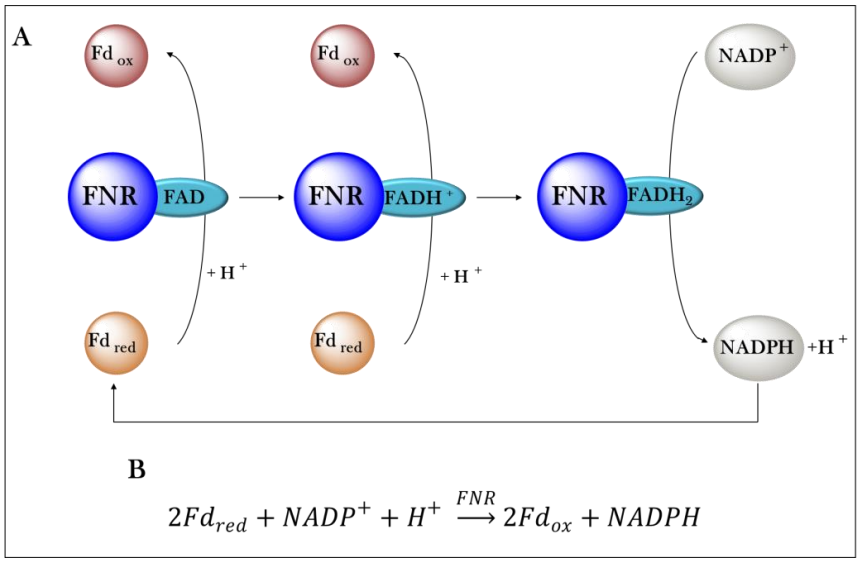

Fig. 10. (A) Diagram of the redox process in which FNR is involved during photosynthesis. (B) Overall reaction catalysed by FNR.

The main structural feature of FNR is that it shows two domains: a flavin-binding domain (more precisely a flavin adenine dinucleotide, FAD) in which the cofactor is accommodated and the $NADP^+$-binding domain which is responsible for the binding of the nucleotide substrate (Fig. 11) (Medina and Gómez-Moreno, 2004).

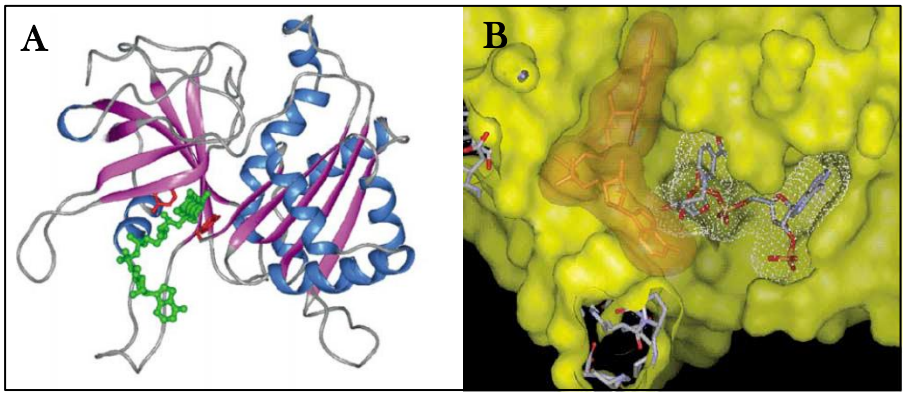

Fig. 11. (A) Tridimensional structure of FNR (PBD: 1QUE). FAD is shown in green sticks. (B) FAD and NADP+ binding sites. The protein surface is shown in yellow and FAD (orange) and NADP+ (shadowed white) are shown in sticks.

The interactions between FNR and its protein partners (Fd and its substitutive flavoprotein Flavodoxin (Fld) in iron-deficient environments) have been extensively studied (Hurley *et al.*, 2006; Medina and Gómez-Moreno, 2004). It is known that both Fd and Fld interact electrostatically with FNR at the same interaction surface, and that the interaction between the former is stronger mainly due to a more specific interaction (Martínez-Júlvez *et al.*, 2009). In order to get a further insight into the physico-chemical properties of these interactions, our group used Dynamic Force Spectroscopy (DFS) to analyse the nanomechanical properties of the protein complexes formed by FNR and found that the mechanical stability of the FNR complex with its natural electron donor, Fd, is almost 3-fold higher and its lifetime longer than in the case of the complex with Fld (Gómez-Moreno and Lostao, 2013; Marcuello *et al.*, 2012; Gómez-Moreno *et al.*, 2011; Marcuello *et al.*, in preparation).

Regarding the interaction of FNR and its enzymatic substrate $NADP^+$, which is the aim of this project, it is known that certain aminoacid residues in the $NADP^+$ binding pocket of FNR interact directly with the 2'-P group of $NADP^+$. In addition, some structural rearrangements in the protein that assure the coenzyme specificity are also needed (Medina and Gómez-Moreno, 2004). We proposed the following working hypothesis: due to the high specificity that the enzyme FNR shows for its enzymatic substrate, $NADP^+$, their interaction in terms of unbinding force for the FNR: $NADP^+$ complex may be stronger than that seen between FNR and its electron donor Fd. With this study, we intend to fully characterize the interactions between FNR and its substrate and protein partners, broadening the extensive knowledge that our group has gather of this enzyme along the years. On the other hand, it should be highlighted that this is the first nanomechanical study on an enzyme-substrate system.

2. OBJECTIVES

These were the objectives proposed at the beginning of the project:

1. Immobilize the protein Ferredoxin-$NADP^+$ Reductase on the surface of flat mica pieces in order to be used for molecular recognition studies preserving its functionality.

2. Design a reproducible protocol for the immobilization of nicotine adenine-based nucleotides (such as $NADP^+$) on AFM tips for their use as functionalized probes during the force measurements.

3. Study for the first time the molecular recognition process as well as the interaction forces established between the enzyme FNR and its enzymatic substrate $NADP^+$. To that matter, the most probable unbinding force has to be obtained at different loading.

4. To determine the specificity of the binding events obtained in the AFS experiments by means of blocking experiments.

5. To obtain the mechanostability parameters of the FNR:$NADP^+$ complex using the Ritchie-Evans model in order to be able to elucidate the energy landscape of the complex.

3. MATERIALS AND METHODS

3.1. Protein labelling

The protein FNR from *Anabaena* PCC 7119 was purified from *Escherichia coli* BL21 cultures in the Biochemistry and Cellular and Molecular Biology Department of the University of Zaragoza by Dr. Marta Martínez Júlvez. Then it was labelled using the heterobifunctional crosslinker sulfo-LC-SPDP (sulfosuccinimidyl 6-[3'(2-pyridyldithio)-propionamido] hexanoate; Pierce) (Fig. 12). This crosslinker contains an amine-reactive end, an N-hydroxysuccinimide (NHS) ester group, that binds to primary amines (-NH_2) from the lateral chain of lysine residues at the surface of FNR. The other terminal group (a 2-pyridyldithiol group) is a sulfhydryl-reactive portion which reacts optimally with sulfhydryl groups resulting in displacement of a pyridine-2-thione molecule and the formation of a disulfide bond.

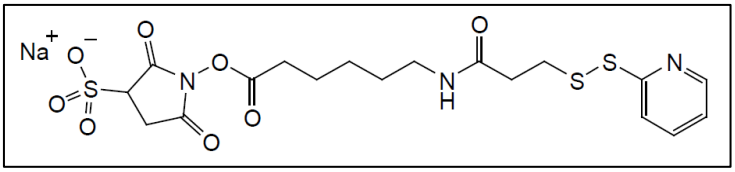

Fig. 12. Sulfo-LC-SPDP crosslinker.

These are the steps followed for the FNR labelling:

1) *SPDP binding to FNR*: A fresh 20mM SPDP solution in 50 mM Tris-HCl, pH 8 was prepared. Then 15 µl of this solution were added per milligram of protein to be labelled. This solution was incubated during 50 min at room temperature under mild stirring. The reaction produces tagged-species of free FNR carrying a C_9-long arm ending in a 2-pyridyldithiol group (FNR-PDP) (Fig. 13).

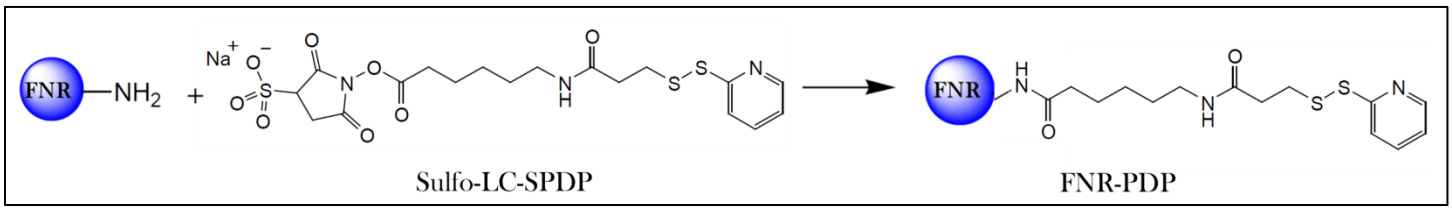

Fig. 13. Reaction of the amine groups on the surface of FNR with the NHS group from SPDP to yield labelled FNR (FNR-PDP).

2) *FNR-PDP purification*: FNR-PDP molecules were isolated from unreacted SPDP and other molecules and concentrated using a Microcon-10kDa Centrifugal Filter Unit. Centrifugation was performed at 4 ºC and 4000 rpm during 15 minutes.

3) Finally, the concentrated protein was resuspended in 50 mM Tris-HCl, pH 8, quantified and stored at -20 ºC.

3.2. FNR-PDP spectrophotometric quantification

The protein concentration was quantified using a Cary 100Bio spectrophotometer from Varian and quartz cuvettes.

Spectra acquisition of free and labelled FNR (FNRwt and FNR-PDP respectively) as well as the base line correction were performed in 50mM Tris-HCl, pH8 using a scan rate of 50 nm/min and a wavelength range between 200 and 800 nm.

According to the Lambert-Beer law, the absorbance of a substance at a certain wavelength can be related to the concentration of that substance in the cuvette as long as the absorbance is kept as a linear function of the concentration. It is known that FNR has a characteristic absorbance peak at 458 nm (Medina and Gómez-Moreno, 2004) and therefore, knowing its molar absorption at this wavelength, FNR concentration can be calculated:

$$Abs_{458} = \varepsilon \cdot C \cdot l \quad \text{(Eq. 6)}$$

ε being the molar absorption coefficient of FNR at 458 nm (9.4 $mM^{-1}cm^{-1}$), *C* the concentration of FNR in the cuvette and *l* the path length (1 cm).

Once the protein was labelled and quantified, it was again filtered using a Microcon-10kDa Centrifugal Filter Unit. Centrifugation was performed at 4 ºC and 4000 rpm during 15 minutes. Then the protein was stored in phosphate buffer saline (PBS) at -20 ºC.

3.3. Enzymatic activity measurements

In order to determine if the labelling and functionalization process affects functionality and enzymatic activity of FNR, kinetic measurements were performed using both free and labelled protein in solution.

A great variety of enzymatic activities have been described for FNR. Among them, the cytochrome *c* reductase (cyt *c*) activity is one of the most used in order to describe the catalytic activity of FNR. Taking advantage of the fact that cytochrome *c* of mammals reduces Fd quite fast, this activity can be measured by monitoring the absorbance increment at 550 nm, being the molar absorption coefficient of cytochrome *c* at this wavelength around 20 $mM^{-1}cm^{-1}$.

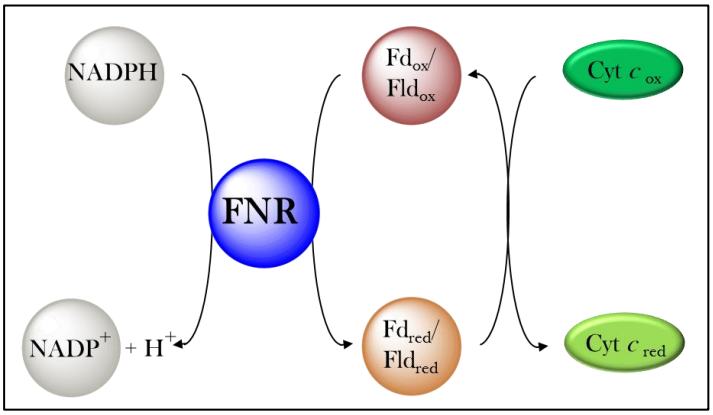

Fig. 14. Electronic transference steps described for the cytochrome *c* reductase.

The activity measurements were performed in a Cary 100Bio spectrophotometer from Varian. The reaction volumes used for these assays and the starting concentrations are shown in table 1. The measurement has to be taken half a minute after all reactants have been mixed. Although FNR may directly reduce some types of cytochrome such as cytochrome *f* (Zanetti and Forti, 1966), it is very inefficient reducing cytochrome *c* from mammals when Fd is absent. This is the reason why Fld or Fd have to be added latest into the cuvette.

Reactives	Reference	FNRwt	FNR-PDP
50 mM Tris-HCl, pH8	900 µl	648 µl	648 µl
Cyt c (7.5 mg/ml)	100 µl	94 µl	94 µl
NADPH (2 mM)	-	121 µl	121 µl
Fld (0.47 mM)	-	137 µl	137 µl
FNR (4 µM)	-	1 µl	1 µl

Table 1. Reaction volumes used for the enzymatic activity measurements in solution.

In order to be able to calculate the turnover number (TON), also known as k_{cat}, the slope of the graphs obtained at 60 s has to be extrapolated.

3.4. FNR-PDP immobilization on mica

Freshly cleaved square muscovite mica pieces (Electron Microscopy Sciences) of approximately 1 cm wide were used as the functionalization substrate for FNR immobilization. Mica is a silicate that can be exfoliated very easily showing afterwards a nanometrically flat surface which is extremely important for AFM topography imaging.

These cleaved mica pieces were fixed on 6-well ELISA *Nunclon Surface* plates (Nunc) in order to proceed with the functionalization process. A scheme of the process can be seen in figure 15:

1) *Mica amination*: Cleaved mica pieces were exposed to APTES (3-aminopropyltriethoxysilane; Sigma-Aldrich) and Hünig's Base (N,N-diisopropylethylamine; Sigma-Aldrich) vapors in a 3:1 volume ratio under argon atmosphere for 2 hours.
   After these two hours, APTES has vaporized and covalently bond to the hydroxyl groups on the mica surface.

2) *SPDS binding to mica-NH_2 pieces*: Fresh 20 mM SPDP in deionized water was prepared and diluted 20 times in PBS-EDTA-azide pH 8.3 (ethylenediaminetetraacetic acid; Pierce). 200-300 µl of the final solution were added to each mica-NH_2 piece and incubated for 50 minutes at room temperature without stirring. After incubation, mica pieces were washed three times (5 min each) using the same incubation buffer.
   During this time the NHS group of the SPDP binds to the amines on the surface of the mica leaving a reactive group at the other end of the crosslinker (mica-PDP).

3) *PDP reduction*: The exposed PDP groups on the mica pieces were reduced with 3 ml of 150 mM DTT (dithiothreitol; Sigma-Aldrich) in PBS-EDTA-azide pH 8.3 at 4 ºC during 30 min under stirring. After incubation, mica pieces were washed three times (5 min each) with PBS-EDTA pH 8.3.

4) *FNR-PDP binding to the mica-SH surface*: Different amounts of FNR-PDP were added to the wells (from 0.6 to 15 µg) in order to determine the proper amount of protein needed for obtaining a homogenous layer. The protein was incubated overnight at room temperature under stirring in the absence of light.
   Finally, mica pieces were washed three times using PBS, 0.2% Tween 20 (Panreac) and 0.1% SDS (Panreac) pH 8.3 to remove unbound proteins and kept in PBS pH 8.3 at 4 ºC in the absence of light until further use.

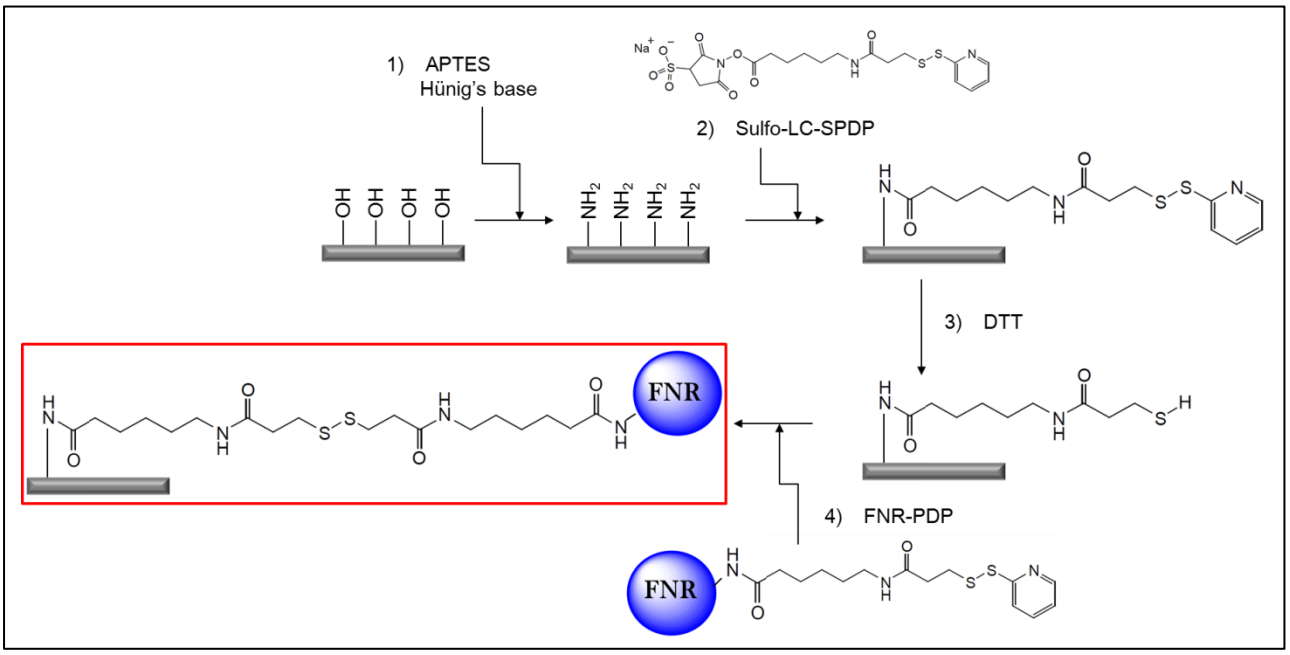

Fig. 15. Functionalization process of FNR on the mica surfaces.

3.5. AFM topography and *scratching*

AFM topography images were obtained in a MultiMode 8 AFM (Bruker Digital Instruments, Santa Barbara, USA) using MSNL-10 tips (Bruker Probes) with spring constants, *k*, of 0.03, 0.1 and 0.6 N/m (Fig. 16). These are tips on a nitride cantilever with a final tip radius of 2 nm approximately. In this case the bare tip was used to obtain only topography images.

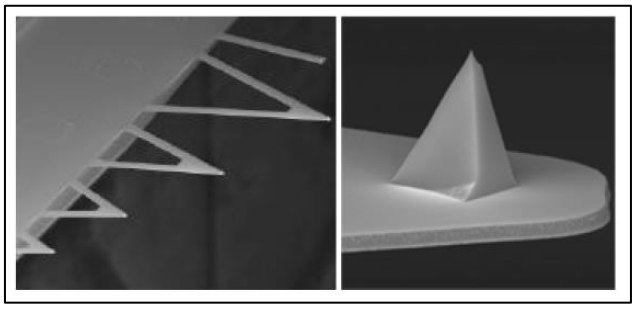

Fig. 16. Scanning electron microscopy images of MSNL cantilevers and a tip. The cantilevers used were the smallest ones, being their spring constants (from left to right) 0.6, 0.1 and 0.01 N/m respectively.

Images were acquired in tapping mode making the cantilever to oscillate near its respective resonant frequency (between 7 and 15 kHz). As the subject of study is a biological system, all measurements were performed in a liquid cell using PBS pH 8.3 to mimic physiological conditions. Figure 17 shows the liquid cell used. The analysis of the images was done using WxSM 5.0 free software for SPM (Horcas *et al.*, 2007).

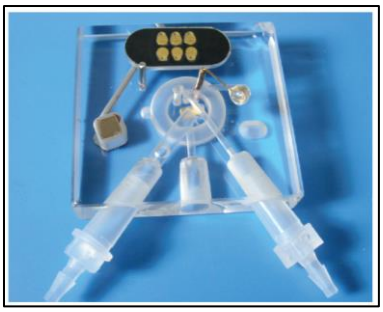

Fig. 17. Liquid cell used in the MultiMode 8 system.

In general terms, the smaller the spring constant, the more sensitive the measurements are regarding to changes in topography which means that greater resolution can be achieved using them. This is why the softest cantilevers were used to obtain the topography images and the hardest one (0.6 N/m) was used for *scratching*. This technique consists on moving the tip over the sample in contact mode, dragging the functionalized groups throughout the surface (Jiang *et al.*, 2011). By controlling the normal force applied to the probe, patterns can be fabricated and the mica surface can be uncovered so that a clear height profile can be obtained.

3.6. AFM tip functionalization

In order to perform the force measurements, different probes than those used for the topography images acquisition have to be used. The main difference is that these probes now have to be functionalized. Prefunctionalized probes were purchased from Novascan Technologies Inc. (Ames, USA). Two different type of probes were used, one with a triangular shape and a spring constant of 0.06 N/m and other with a rectangular shape with a spring constant of 0.02 N/m. The cantilevers were calibrated using the thermal noise method (Huttler and Bechhoefer, 1993) in order to calculate their effective spring constant after functionalization.

These AFM probes are coated with a 30 nm-wide gold layer and their tips are modified with a maleimide terminated poly(ethylene)glycol (MW 3400) (PEG) linker that is 20 nm long when it is fully stretched. This spacer will allow to discern which peaks in the force-distance curves are due to specific interactions between the receptor on the surface and the ligand on the tip (enzyme and enzymatic substrate respectively in this study) and those peaks due to non-specific cantilever-sample interactions.

As mentioned before, one of the objectives of this project was to develop a reproducible protocol for the functionalization of AFM tips with $NADP^+$. This was done by means of another

crosslinker, Traut's Reagent (2-iminothiolane; Pierce) (Fig. 18). This is a cyclic thioimidate compound used for thiolation. It reacts with primary amines and introduces a sulfhydryl group.

The subsequent steps were followed in order to covalently attach $NADP^+$ molecules to the AFM tip (Fig. 18):

1) *Incubation of $NADP^+$ and Traut's Reagent*: A 2 mg/ml Traut's Reagent solution in PBS-EDTA 5mM, pH 7.2 was prepared. A different pH is used in this process because at pH greater than 7.5, maleimide can hydrolyse. One mole of $NADP^+$ (nicotinamide adenine dinucleotide phosphate; Sigma-Aldrich) per 10 moles of Traut's Reagent was added to the mixture and incubated during 2 hours at room temperature in the absence of light.

2) *Tip incubation*: After 2 hours, 150-200 µl of the reaction mixture were added to the tip fixed on a capsule and incubated overnight at 4 ºC in the absence of light.
   Finally, the tip was washed three times (5 min each) with the same incubation buffer and kept at 4 ºC in the absence of light until use.

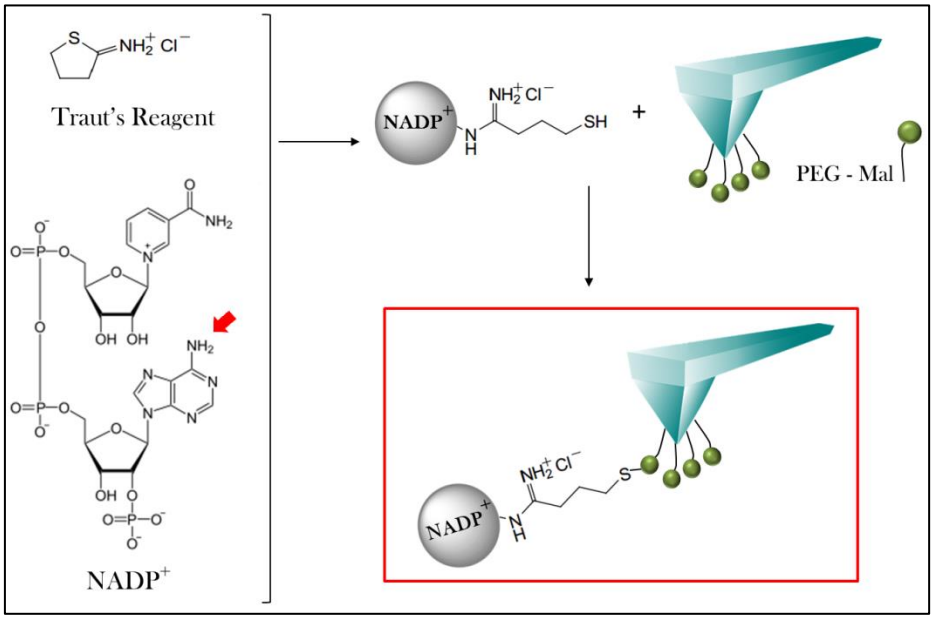

Fig. 18. Scheme of the tip functionalization process.

3.7. AFS experiments

Force spectroscopy measurements were performed with a MultiMode 8 AFM (Bruker Digital Instruments, Santa Barbara, USA) using a PicoForce spezialized Scanner (Fig. 19). This scanner allows to measure ultra-sensitively very small forces. The measurable range of forces is approximately between 1 pN and 10 mN. This scanner controls the tip-sample separation with a piezoelectric device within a 20 μm of range. In addition, the MultiMode PicoForce allows moving the tip in the X-Y plane relative to the sample within a range of 40 μm^2.

Fig. 19. PicoForce Control Module, PicoAngler and MultiMode Scanning Probe Microscope (SPM).

Several hundred curves were obtained for $NADP^+$-cantilever/FNR-mica interactions at different loading rates. Force-distance curves (Fz curves) were obtained applying a voltage to the z-piezo (picoforce scanner) at a tip-retraction velocity ranging from 50 to 4000 nm/s which translates into loading rates (*R*) of 3 to 80 nN/s. The curves were collected as voltage versus distance plots. Then the voltage values were translated into force data using the slope of the retraction curve and the calibrated values of the spring constants of the functionalized cantilevers. The loaded force between the tip and the sample was kept constant at 1.25 nN. The measurements, as mentioned before, were performed in a liquid cell using PBS pH 7.2 at room temperature.

Negative control experiments, called blocking experiments, were carried out by blocking the available $NADP^+$ binding sites in the immobilized FNR incubating the sample with 2.6 mM $NADP^+$ during 15 min. Fz curves were then obtained only at a loading rate of 10 nN/s.

After the measurements, histograms were built for each loading rate in which the percentage of specific events was represented versus the rupture force. These histograms were built using only the specific events recorded in the Fz curves: those that show a matching distance with the stretched linker length and a profile that reflects the stretching of the flexible linker (Hinterdorfer *et al.*, 2000). Then histograms were fitted using a Gaussian function in order to obtained the most

probable unbinding force for a single rupture event (F^*). Finally the mechanostabilty parameters k_{off} (dissociation rate constant in the absence of any external force) and x_β (the distance between energetic barrier of the reactants and the transition state) are obtained using the Bell-Evans model (Bell, 1978; Evans *et al.*, 2001) as explained in section 1.2.2.

4. RESULTS

4.1. Protein labelling and functionalization

The objective for tagging the protein with a crosslinker is to immobilize it onto a flat mica surface in order to perform force measurements using an AFM. Protein immobilization in a functional active form is fundamental for its activity. Exceptionally, a methodology for a controlled and oriented FNR immobilization towards its protein partners was pursued, as previously developed by our group in which the binding site of FNR protein partners was protected during the labelling process. This allowed to largely increase the effectiveness in AFS (Marcuello *et al.*, 2012). However, in this work, as usual in AFS, a random labelling was performed due to the fact that in this case the interaction we were interested in studying was that between FNR and its substrate $NADP^+$ whose binding site defers from that of FNR protein partners. The results, in terms of percentage of tip approaches that produced specific events, obtained using a random labelling and attachment ranged between 4 and 18%. These data are similar to those found in the literature for this kind of experiments using random procedures.

With the purpose of assuring the integrity of the tagged species of FNR, a steady-state enzymatic assay was performed as explained in section 3.3 in which the cytochrome *c* reductase activity in solution of labelled FNR (FNR-PDP) was compared to that of the free enzyme (FNRwt) (Fig. 20).

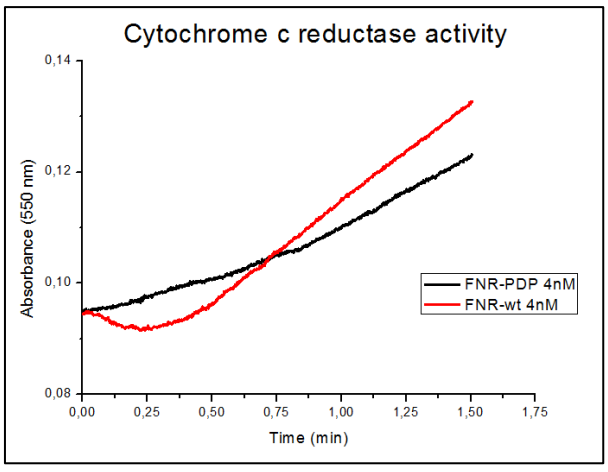

Fig. 20. Cytochrome *c* reductase activity assay results. As seen, the enzymatic activity of FNRwt reached higher values in terms of absorbance at 550nm after one and a half minutes.

The catalytic activity of an enzyme is measured in terms of its turnover number (TON), also known as k_{cat}, and it is defined as the number of molecules that the enzyme converts into product per catalytic site per unit of time.

FNRwt exhibited a TON value of 7.56 s^{-1} while FNR-PDP showed a rate of 5.08 s^{-1} (Table 2). All measurements were performed at a FNR concentration of 4 nM that is the usual concentration for measuring FNR activity in solution. Although there is a 1.5-fold decrease of the turnover number in labelled FNR with respect to free FNR, the steady-state enzymatic assay gave positive data showing, on the one hand, that the functionality of the samples was only slightly affected by the tagging process and, on the other hand, that the enzyme is still able to recognize and bind efficiently to its substrate. This concurs with previous results in our group which showed that random labelling processes always affects enzyme activity somehow (Marcuello *et al.*, 2012).

Sample	Δ Abs (mUA)	[FNR] (nM)	TON, k_{cat} (s^{-1})
FNR wt	0.03629	4	7.56
FNR-PDP	0.02439	4	5.08

Table 2. Kinetic parameters of FNR-PDP for cytochrome *c* reductase activity.

4.2. AFM imaging

AFM imaging was used as a tool to monitor the results of the immobilization process of FNR on the surface of flat mica pieces at a molecular level. Topography images showed that the enzyme forms a homogeneous monolayer when at least 4 µg of protein were added to each mica piece of approximately 1 cm^2. (Fig. 21). The rest of the functionalizations were performed adding 4 µg of protein to each mica piece.

Topography images of the functionalized mica surfaces show a height between 8 and 12 nm (Fig. 21 and 22). This height is consistent with the expected length of the reaction products used during the functionalization and coincides with that obtained in the scratching profile (Fig. 22B).

Another aspect of the functionalized mica worth mentioned is that the layer, as imaged by AFM, is not regular but it rather displays mounts and valleys randomly distributed over the surface.

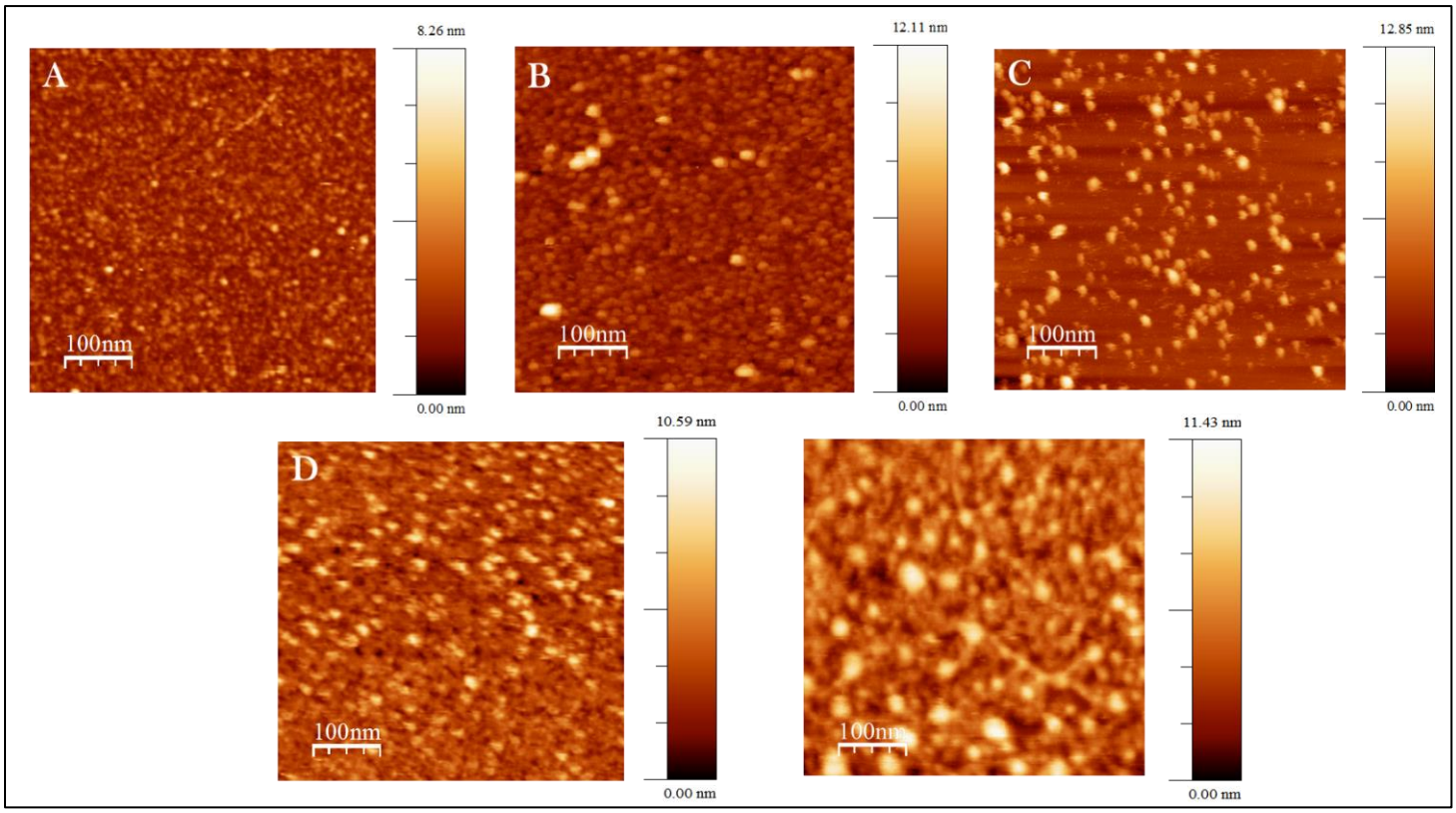

Fig. 21. AFM topography images of functionalized mica with different amounts of FNR. (A) 1 µg, (B) 1.5 µg, (C) 2 µg, (D) 4 µg and (E) 6 µg. A homogenous monolayer appears when at least 4 µg of FNR are added.

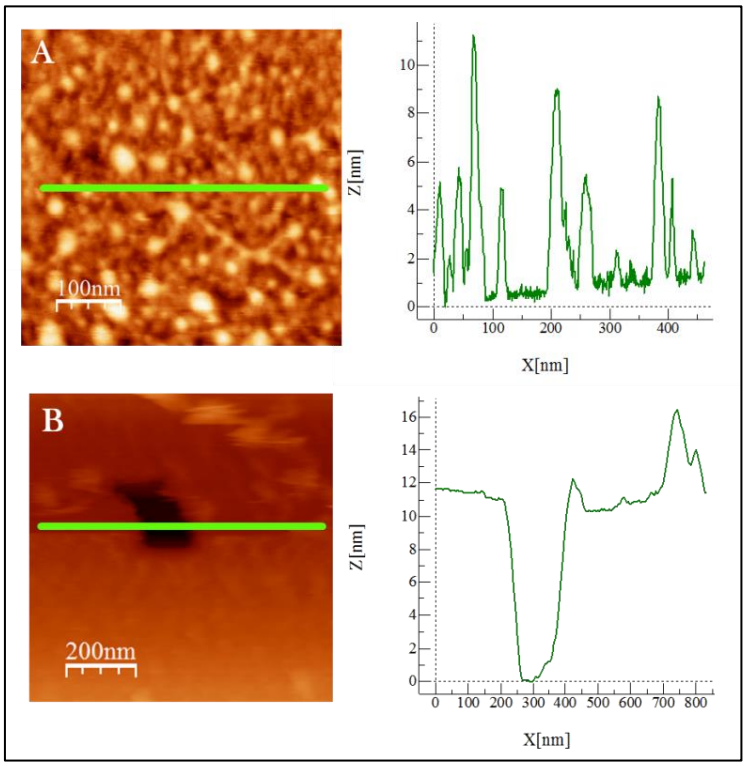

Fig. 22. (A) Distribution of FNR-PDP covalently bond on mica and the corresponding height profile showing a maximum height of 11.43 nm. (B) Scratching on the functionalized mica and its height profile showing a maximum height between 11 and 12 nm.

4.3. Force Spectroscopy

Force data from the analysis of the force-distance curves were obtained as explained in section 3.7.

A typical mica-FNR:NADP$^+$-tip force scan is depicted in Figure 23. Starting from the zero-force point, the tip is moved closer to the sample with an increment in the force (blue line) until tip and sample come into contact. Pushing the tip further towards the surface requires higher forces causing the bending of the cantilever. Retraction of the tip (red line) produces a sharp jump (the peak seen in the curve) indicating that a sudden release has occurred between the tip and the sample. This is due to the rupture of the bond between the two interacting molecules (f_u). The specific length of the peak (l_u), coincident with that of the stretched maleimide-PEG linker (approximately 20 nm), indicates that the force, f_u, can be attributed to a specific event.

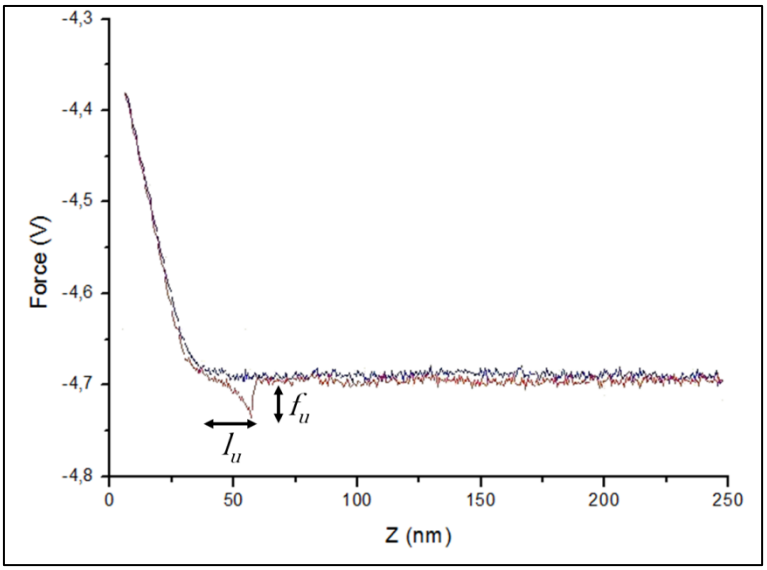

Fig. 23. Force curve showing a single specific event for a FNR:NAPD$^+$ complex. Molecules are brought into contact when the tip is moved towards the sample (blue line). In the retraction line (red line) the force unbinding force required is shown (f_u). The total length at which the unbinding occurs (l_u) is defined as the unbinding length.

Figure 24 shows the histograms built at the four different loading rates used in the measurements. Each histogram represents the relative frequency (in terms of percentage) of specific unbinding events versus the unbinding force. As it can be seen, data in all histograms can be fit under two peaks. The first peak indicates the relative frequency of events that occur at the displayed force and accounts for those interactions in which a single FNR molecule interacts with a single NADP$^+$. Those rupture events observed at higher force values are the ones in which two proteins on

the mica are binding to two different $NADP^+$ molecules on the AFM tip. This is the reason why the second peak appears at force values that are double of those for the single event.

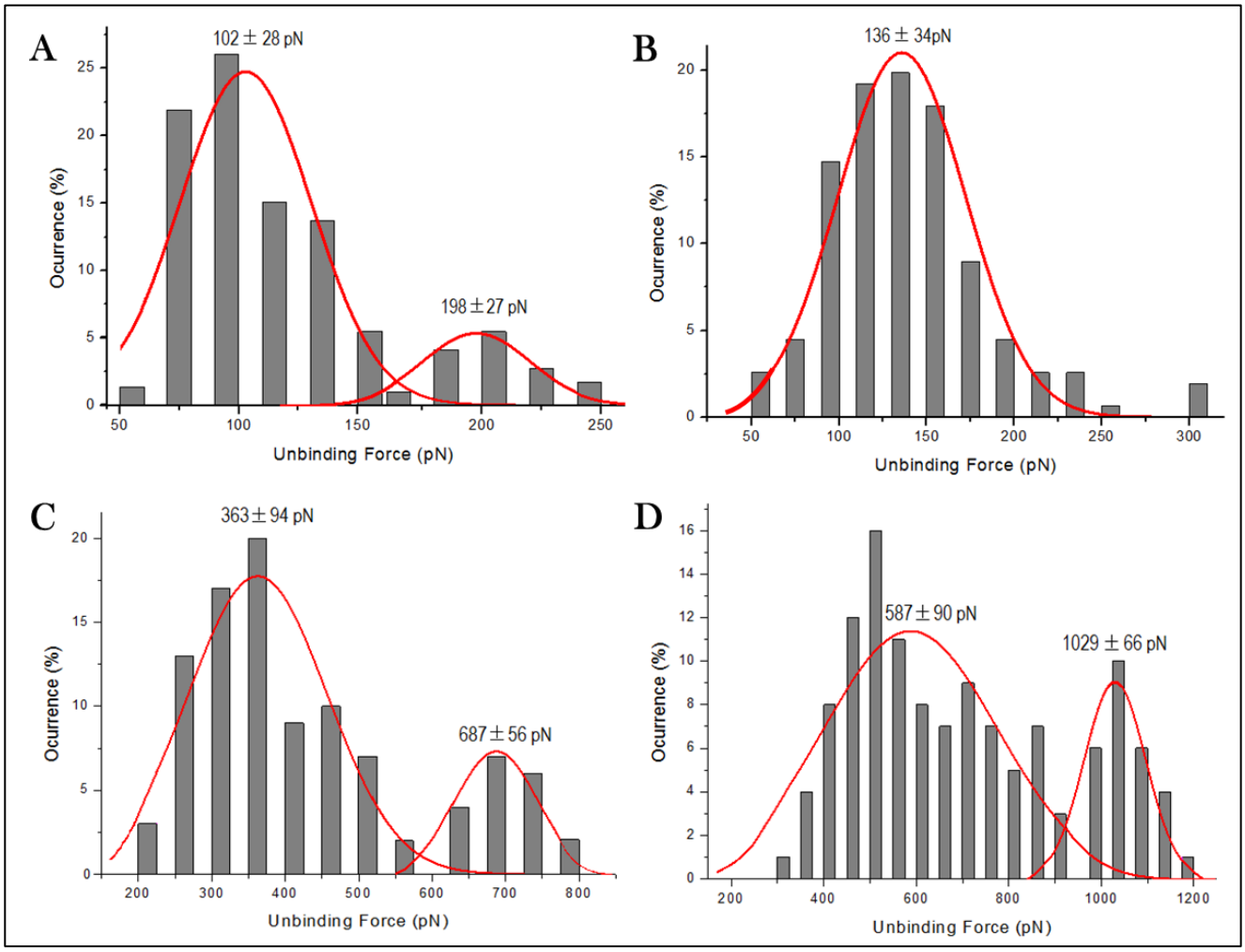

Fig. 24. Force distributions obtained at loading rates of 6 (A), 10 (B), 20 (C) and 78 nN/s (D) for the FNR:$NADP^+$ complex. The most probable unbinding force is indicated for each distribution.

The results show that the bond probability increases with the loading rate for the FNR:$NADP^+$ complex, as more multiple events are seen at higher velocities. This suggests that the faster the tip approaches to the surface the more it favours the formation of bonds between the enzyme and its substrate, thus the number of multiple events increases. It is worth mentioned that at a loading rate of 10 nN/s (Fig. 24B), the second peak is too small to be statistically significant, however, it follows the tendency of multiple events appearing at every loading rate. The fact that multiple events are so uncommon at this loading rate may indicate that this is the optimal loading rate for this complex under the conditions it was tested.

Regarding the force data, the intermolecular forces fall into the expected trend considering the fact that the most probable unbinding force increases with the loading rate. The corresponding mean rupture forces, obtained by fitting the histograms to a Gaussian function, were 102±28 pN (R = 6 nN/s), 136±34 pN (R = 10 nN/s), 363±94 pN (R = 20 nN/s) and 587±90 pN (R = 78 nN/s),

Both the specificity of the interaction probed in this experiment and the quality of the experimental design were evaluated by means of blocking experiments at a loading rate of 10 nN/s, as it has been stated as the standard loading rate for biological complexes. These results are summarized in Figure 25. Very similar data was observed between the blocked and the non-blocked samples in terms of the most probable unbinding force, as shown in the Figure. This indicates that both interactions are within the same range of forces assuring the quality of the experiment. Moreover, as expected, the rupture events frequency decreases (from 18 to 4%) for the blocked sample indicating the specificity of the forces recorded.

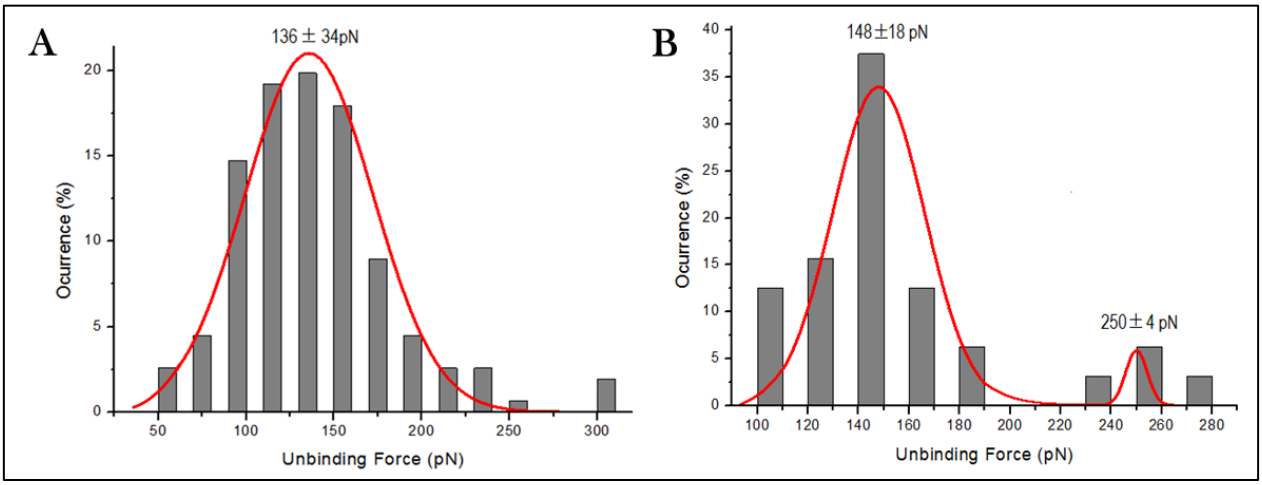

Fig. 25. Force distributions for the non-blocked (A) and the blocked (B) samples obtained at a loading rate of 10 nN/s.

4.4. Dissociation kinetics for the FNR:NADP$^+$ complexes

The energy landscape of a bond rupture explored by AFS defines the force-driven pathway along the pulling direction until the bond rupture. A typical energy landscape is a one-dimension plot representing the energy of the system versus the reaction coordinates (Kramers, 1940). The shape of this landscape is thus constituted by the height of the energy barrier and the energy barrier width between the valley and the summit of the peak. The height of the energy barrier is characterized by the k_{off} value, whereas the energy barrier width is described by the x_β parameter.

In order to calculate both values, the most probable unbinding force is represented as a function of the loading rate (Fig. 26). This plot exhibits one linear regime. Such behaviour can be traced back to the presence of one intermediate state in the dissociation process of FNR and $NADP^+$ (Strunz *et al.*, 1999). This means that $NADP^+$ dissociates from FNR through a single energy barrier between the initial and the transition state of the highest energy to which the system must be raised before dissociation can occur. The k_{off} and x_β parameters can be then extracted from the linear fit.

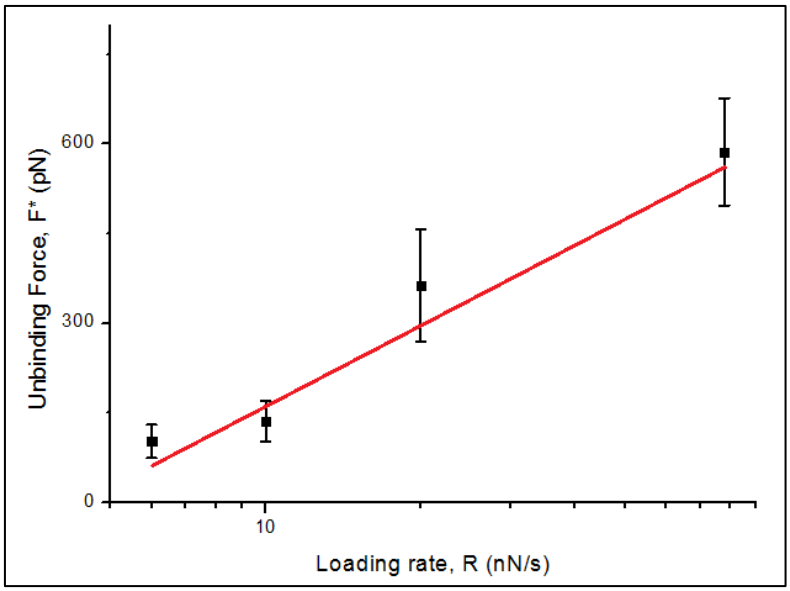

Fig. 26. Loading rate dependence on the most probable unbinding forces.

This indicates that a single energy barrier is crossed during the unbinding process (Yuan *et al.*, 2000). According to Evans theory (Evans and Ritchie, 1997), by applying a linear force on the bond, the energy landscape is tilted such that the energy barrier is reduced.

Fitting the *F** versus *lnR* plot with equation 5, gives both kinetic parameters at zero force conditions (x_β and k_{off}) by relating to the slope and the intercept of the linear fit, respectively. Table 3 summarizes the kinetic parameters of the dissociation of the FNR:$NADP^+$ complex obtained from the fitting of data in Figure 24.

	Unbinding Force for a Single Complex (pN)	k_{off} **(s^{-1})**	τ **(s)**	x_β **(nm)**
FNR:$NADP^+$	136±34	0.0198	50.6	0.0205

Table 3. Mechanical parameters obtained for the dissociation of FNR:$NADP^+$ complex from fitting data shown in Figure 26. The intermolecular force for a single complex was measured at R 10 nN/s.

The analysis gave a position the energy barrier along the reaction coordinate, x_β, of 0.0205 nm. The calculated k_{off} value was of 0.0198 s^{-1}. This value is related to the characteristic lifetime, τ_o, of the complex ($\tau_o = k_{off}^{-1}$). The expected life for this complex is 50.6 s. This data provides information on the specificity of the reaction: it is thought that a greater half-time is associated with greater specificity in the biorecognition process (Robert *et al.*, 2007).

5. DISCUSSION

During this Master Project the interaction forces between an enzyme and its enzymatic substrate were studied at a single molecule level for the first time using AFS.

The biological complex chosen was the FNR-$NADP^+$ system that is involved in the last step of the photosynthesis light reactions in plants, algae and cyanobacteria. Our group has been involved in many studies of this enzyme as it belongs to a large family of proteins called flavoproteins, one of the main research areas of our group. In previous works, the interaction of FNR with its protein partners, Fd and Fld, and its substrate, $NAPD^+$ has been extensively studied using classical biochemistry techniques. However, these methods provide average signals and behaviour of the total of molecules involved in the study. AFS was used in our group to define the energy landscape and the mechanostability parameters of the dissociation of FNR from both its protein partners so this project fulfils the characterization of all the interactions of FNR at the single molecule level.

A typical AFS experiment requires the immobilization of the interacting partners, one on the surface of a substrate and the other one at the AFM tip. In this work the enzyme FNR was immobilized on the surface of flat mica pieces. It is of pivotal importance that both the labelling process and the immobilization process have no effect over the functionality and the catalytic activity of the enzyme. To monitor this, two different control experiments were carried out. On the one hand, the absorbance spectrum of the enzyme was checked after the labelling process. The characteristic peak of FNR appeared at 458 nm, assuring that the structure of the FMN center of the enzyme was not affected by this process.

On the other hand, the catalytic activity of the enzyme after the tagging process was compared to the catalytic activity of the wild type one by monitoring the cytochrome *c* reductase activity. Although the activity of the labelled FNR exhibited a 1.5-fold decrease with respect to the free FNR (Table 2), it still had high catalytic activity. This steady-state enzymatic analysis showed that the labelled FNR was still able to bind to its substrate, proving the suitability of this labelling process for our final purpose.

AFM imaging was used to control the immobilization of FNR on the mica surfaces. Images taken in tapping mode in fluid showed that a monolayer of FNR appeared when at least 4 µg of protein were added to each single mica piece. Topography images (Fig. 21) revealed the typical features of a protein monolayer. It is not a perfectly homogeneous monolayer but it displays

proteins molecules that appear as bigger and brighter circles in the images that are due to the globular shape of this protein and some holes. The height profiles seen in the functionalized mica pieces agreed with those found in other similar studies (Fig. 22). The scratching experiment confirmed that the total height of the functionalization product was around 12 nm. The height profile obtained in the scratching experiment is more accurate than the profile obtained in any other topography image because in the former, the surface of the mica piece is cleared and the height is measured exactly from the mica surface.

One of the objectives of this project was to develop a reproducible procedure to functionalize $NADP^+$ on surfaces, particularly on AFM tips. This is not a straightforward issue as too many factors have to be taken into account. The most important aspect to be considered is the reaction conditions. We are dealing with organic and biological molecules that are very sensitive to environmental changes, especially proteins, which can lose their structure and activity when pH changes just a few tenths. Another matter worth mentioned is the linker used to bind the ligand to the AFM tip. Although PEG is the most used spacer, there are other ones that can be used too. It is very important to know the stretching and flexibility characteristics of the spacer used because this is what will differentiate a specific event from an unspecific one in the force-distance curves. In our case, we used prefunctionalized tips with PEG ending in a maleimide group to which $NADP^+$ was covalently bond. The presence of PEG allows the identification of the specific events quite easily: those peaks that displayed a non-linear, parabolic-like profile and whose length was around 20 nm.

Typical force spectroscopy experiments were performed on a biological complex system involved in ET processes. The aim of these experiments was to gather further information on the mechanical properties of this specific enzyme-substrate complex and establish the basis for the study of other enzyme-substrate complexes. The experiments consisted in recording multiple force-distance curves obtained by approaching the $NADP^+$ functionalized AFM tip towards the FNR, which is immobilized on the chamber of the AFM instrument.

DFS was applied and several hundreds of force-distance curves were recorded at four different loading rates. From the analysis of the curves, the most probable unbinding force, F*, was obtained for each loading rate (Fig. 24). At a loading rate of 10 nN/s, the most probable unbinding force was of 136 ± 34 pN. When this value is compared to those previously obtained for the interaction between FNR and its protein partners Fd and Fld, 57 ± 19 pN and 21 ± 8 pN respectively (Marcuello *et al.*, in preparation), it can be seen that the mechanical stability exhibited by the FNR:$NADP^+$ complex is clearly higher: almost 3 times higher than the interaction between FNR and Fd and 7

times higher than that between Fld. This was expected as FNR shows greater specificity for $NADP^+$ than for any of its protein partners: FNR can only reduce $NADP^+$ to NADPH but it can accept electrons for this reaction from both Fd and Fld.

It is crucial to evaluate the quality and the specificity of the interactions being recorded during force spectroscopy experiments. Subsequently, to verify if the measured forces could be attributed to specific interaction events between FNR and $NADP^+$, a blocking experiment was performed on the complex. This consists of incubating the protein on $NADP^+$ allowing the binding between them and then performing the force measurements as usual. Now the $NADP^+$ binding pockets in the protein will be occupied so a decrease in the number of specific events is expected proving that previous measurements were in fact specific events. The blocking experiment carried out at only a loading rate of 10 nN/s showed a decrement from 18 to 4 % of such unbinding frequency upon blocking. The significant reduction observed after blocking is clearly indicative of the specificity of the complex formation. The persistence of residual unbinding events has been also reported in other force spectroscopy experiments and could be related to the force interaction between the two partners induced by the experimental setup (Hinterdorfer *et al.*, 1996). Importantly, the force distributions of the unblocked and blocked samples show a good correlation, thus indicating the same nature of the corresponding interactions.

DFS assumes that the bond can be characterized by two key parameters, the natural kinetic off-rate, k_{off}, that defines the lifetime of the bond in the absence of an applied force, and the width of the interaction potential, x_β, which corresponds to the distance from the energy minimum to the transition state (Noy, 2011). To calculate these parameters, the most probable unbinding force was plot versus the natural logarithm of the loading rate (Fig. 26). The increasing value of the most probable unbinding force with the loading force subscribes to Bell's theory that assumes that loading a bond by an external force exponentially amplifies the bond dissociation rate (Eq. 4) (Bell, 1978):

As shown in Figure 26, the force spectrum of the FNR:$NADP^+$ bond revealed one regime within the range of the experimental loading rates. Thus, in accordance to the simple Bell model, the data indicates that the FNR:$NADP^+$ complex overcomes one single transition during its unbinding. This regime may show that $NADP^+$ can associate with FNR in one optimum orientation to transfer electrons in the redox reaction.

The force measurements were used to obtain an estimate of the activation energy barrier between the FNR:$NADP^+$ pair. The results are shown in Table 3. The k_{off} value was estimated to

0.0198 s^{-1} but it is not as high as expected for a ET complex (Huley *et al.*, 2006) such as the complex formed by FNR and its protein partners. The k_{off} values estimated for the FNR:Fd were of 21.2 s^{-1} and for FNR:Fld of 55.7 $s^{-1}$and 235.3 s^{-1} (the complex FNR:Fld showed two distinct linear regimes) (Marcuello *et al.*, in preparation).

The reason for such a difference may lie in the fact that most of the dissociation rate constant values that have been estimated are from protein-protein complexes, not from enzyme-enzymatic substrate complexes. However, these data concur with other off-rates estimated by AFS for stable ligand-receptor complexes, as antigen-antibody pairs that are in the range of 0.01 s^{-1}. Interactions between an antigen and its antibody are very specific interactions with long life times. Time life values obtained here for the FNR:$NADP^+$ complex are very similar to those obtained for the previously mentioned interacting pair. It is said that the greater the half-time of a bond, the greater specificity on the biorecognition process (Robert *et al.*, 2007). This theory together with the results obtained, certifies the high specificity of the interaction between FNR and $NADP^+$ that we stablished as the working hypothesis.

Only a rough estimation has been made of the Bell model parameters for both transitions by fitting the force measurements to the Evans-Ritchie equation (Eq. 5) (Evans and Ritchie, 1997). In order to have a good estimation of these parameters, a minimum of six different loading rates should be used in the experimental part. Due to a lack of time and that the fact that taking these measurements is a very time-consuming process, only four loading rates were used. It is expected that in the future, more measurements at different loading rates will be carried out so that a proper calculation of the mechanostability parameters can be made.

All these results provide new insights into the interactions of the enzyme FNR with its enzymatic substrate, $NADP^+$. However, many things can still be corroborated using this approach. For example, using different FNR mutants in the aminoacid residues that are involved in its bonding to $NADP^+$, their individual relevance and contribution to this complex formation can be unravelled. This will lead to a further understanding of the redox reactions catalysed by FNR. Moreover, this approach may be extrapolated to other biological systems and can greatly enhance our understanding of biomolecular unbinding. This will be the starting point for the development of new therapeutic targets or diagnosing systems.

6. CONCLUSIONS

These are the conclusions reached at the completion of the Master Project:

1. The enzyme FNR was labelled and immobilized on the surface of flat mica pieces. Although a random tagging and immobilization process was carried out, neither processes barely affected the functionality and catalytic activity of the enzyme. The tagging process was proved almost harmless by an enzymatic activity assay (cytochrome *c* reductase activity). It showed that, although the enzymatic activity of the labelled enzyme was reduced 1.5 times respect to the free enzyme, the tagged enzyme still showed a high activity proving that it was still able to bind specifically and efficiently to $NADP^+$. The immobilization process was monitored by AFM imaging in fluid. In order to increase as much as possible the binding efficiency, the formation of a homogeneous monolayer of protein was pursued and achieved for at least 4 µg of protein per mica piece. Due to the globular nature of the enzyme, the monolayer was not a perfect film but some aggregates and holes were seen.

2. A new protocol for the immobilization of $NADP^+$ on AFM tips has been developed. The used tips were prefunctionalized with PEG ending in a maleimide molecule to which $NADP^+$ was covalently bond. This result has been confirmed by the specificity of the force measurements proved by the blocking experiments.

3. Dynamic Force Spectroscopy has been used for the first time to study the interactions between an enzyme and its enzymatic substrate. Force-distance curves have been obtained at four different loading rates and the most probable unbinding forces have been obtained. The results show that FNR binds more specifically to $NADP^+$ than to its protein partners (Fd and Fld).

4. Blocking experiments verify the veracity and the specificity of the force measurements. This is an indirect confirmation that the tip functionalization protocol is valid.

5. From the data abovementioned, the mechanostability parameters were estimated. The complex FNR:$NADP^+$ exhibits a dissociation pathway that occurs through the formation a single intermediate that have to overcome an energy barrier (activation energy). The k_{off} value obtained is much lower than that of other ET complexes. Their values are similar to those of the antigen-antibody pairs, indicating and corroborating the high specificity of this interaction. Nevertheless, more force measurements at different loading rates are needed in order to accurately calculate the mechanostability parameters.

7. REFERENCES

Bell, G.I. 1978. Models for the specific adhesion of cells to cells. *Science* 200 (4342):618-627.

Binning, G.; Quate, C.F. and Gerber, Ch. 1986. Atomic Force Microscope. *Phys Rev Lett* 49(9):930-933.

Bizzarri, A.R. and Cannistraro, S. 2009. Atomic Force Spectroscopy in Biological Complex Formation: Strategies and Perspectives. *J Phys Chem B* 113(52):16449-16464.

Bizzarri, A.R. and Cannistraro, S. 2010. The application of atomic force spectroscopy to the study of biological complexes undergoing a biorecognition process. *Chem Soc Rev* 39:734-749.

Bizzarri, A.R. and Cannistraro, S. 2012. Dynamic Force Spectroscopy and Biomolecular Rcognition. CRC Press.

Bowen, W.R.; Hilal, N. 2009. Basic Principles of Atomic Force Microscopy. In Butterworth-Heinemann (Eds.) *Atomic Force Microscopy in Process Engineering. Introduction to AFM for Improved Processes and Products*. (1-30). Elsevier Ltd.

Cappella, B. and Dietler, G. 1999. Force-distance curves by atomic force microscopy. *Surf Sci Rep* 34:1-104.

Evans, R. and Ritchie, K. 1997. Dynamic strength of molecular adhesion bonds. *Biophys J* 72:1541-1555.

Evans, E.; Leung, A.; Hammer, D. *et al*. 2001. Chemically distinct transition states govern rapid dissociation of single L-selection bonds under force. *PNAS* 98:3784-3789.

Floring, E.L.; Moy, V.T: and Gaub, H.E. 1994. Adhesion forces between individual ligand receptor paris. *Science* 264:415-417.

Giessibl, F.J. 2003. Advances in atomic force microscopy. *Rev Mod Phys* 75:949-983.

Gómez-Moreno, C.; Marcuello, C.: de Miguel, R. et al. 2011. Atomic Force Microscopy as tool to understand the Mechanoestability of Ferredoxin-$NADP^+$ reductase Complexes with its partners. In Miller, S.; Hille, R. and Palfey, B. (Eds.). *Flavins and Flavoproteins*. (17:569-575). Lulu.com.

Gómez-Moreno, C. and Lostao, A. 2013. Single Molecule Methods to Study Flavoproteins. In Hille, R.; Miller, S. and Palfey, B. (Eds.) *Handbook of Flavoproteins: Volume 2, Complex Flavoproteins, Dehydrogenase and Physical Methods*. (12:297-318).

Hinterdorfer, P.; Baumgartner, W.; Gruber, H.J. *et al*. 1996. Detection and localization of individual antibody antigen recognition events by atomic force microscopy. *Proc Natl Acad Sci USA*. 93:3477-3481.

Hinterdorfer, P.; Schilcher, K.; Baumgartner, W. *et al*. 1998. A mechanistic study of the dissociation of individual antibody-antigen pairs by atomic force microscopy. *Nanobiology* 4:39-50.

Hinterdorfer, P.; Kienberger, F.; Raab, A. *et al*. 2000. Poly(Ethylene Glycol): An Ideal Spacer for Molecular Recgonition Force Microscopy/Spectroscopy. *Single Mol* 2:99-103.

Hinterdorfer, P. and Dufrêne, Y.F. 2006. Detection and localization of single molecular recognition events using atomic force microscopy. *Nature Med* 3(5):347-355.

Horcas, I.; Fernández, R.; Gómez-Rodríguez, J.M. *et al*. 2007. WSxM: a software for scanning probe microscopy and a tool for nanotechnology. *Rev Sci Instrum* 78:013705.

Hurley, J.K.; Tollin, G.; Medina, M. *et al*. 2006. Electron transfer from ferredoxin and flavodoxin to ferredoxin-$NADP^+$ reductase. In Golbeck, J.H. (Ed). *Photsystem I: The light-driven plastocyanin: ferredoxin oxidorreductases*. (445-476). Springer.

Hutter, J.L. and Bechhoefer, J. 1993. Calibration of atomic-force microscope tips. *Rev Sci Instrum* 64:1868-1873.

Jelesarov, I. and Bosshard, H.R. 1994. Thermodynamics of Ferredoxin Binding to Ferredoxin-NADP(+) Reductase and the role of water at the complex interface. *Biochemistry* 33(45):13321-13328.

Jiang, X.; Wu, G.; Zhou, J. et al. 2011. Nanopatterning on silicon surface using atomic force microscopy with diamond-like carbon (DLC)-coated Si probe. *Nanoscale Research Letters* 6:518.

Kramers, H.K. 1940. Brownian motion in field of force and the diffusion model of chemical reactions. *Physica VII* 284-304.

Lee, G.U.; Chrisey, A.C. and Colton, R.J. 1994. Direct measurements of the forces between complementary strands of DNA. *Science* 266:771-773.

Lee, G.U.; Kidwell, D.A. and Colton, R.J. 1994. Sensing discrete streptavidin-biotin interactions with atomic force microscopy. *Langmuir* 10:354-357.

Marcuello, C.; de Miguel, R.; Gómez-Moreno, C. *et al*. 2012. An efficient method for enzyme immobilization evidenced by atomic force microscopy. *Protein Eng Des Sel* 25:715-723.

Marcuello, C.; de Miguel, R.; Martínez-Júlvez, M. *et al*. Mechanostability of the electron-transfer complexes between Anabaena Ferredoxin-$NADP^+$ Reductase and its redox protein partners studied by single molecule techniques. *In preparation*.

Martínez-Júlvez, M.; Medina, M. and Velázquez-Campoy, A. 2009. Binding Thermodinamic of Ferredoxin $NADP^+$ Reductase: Two different protein Substrates and One Energetics. *Biophys J* 96:4966-4975.

Medina, M. and Gómez-Moreno, C. 2004. Interaction of ferredoxin-$NAPD^+$ reductase with its substrates: optimal interaction for efficient electron transfer. *Photosynthesis Research* 79:113-131.

Noy, A. 2011. Force spectroscopy 101: how to design, perform, and analyse an AFM-based single molecule force spectroscopy experiment. *Current Opinion in Chemical Biology* 15:710-718.

Robert, P.; Benoliel, A.M.; Pierres, A. *et al*. 2007. What is the biological relevance of the specific bond properties revealed by single-molecule studies? *J Mol Recognit* 20(6):432-447.

Strunz, T.; Oroszlan, K.; Schäfer, R. *et al*. 1999. Dynamic force spectroscopy of single DNA molecules. *Proc Natl Acad Sci USA* 96:11277-11282.

Yuan, C.; Chen, A.; Kolb, P. *et al*. 2000. Energy Landscape of Streptavidin Biotin Complexes Measured by Atomic Force Microscopy. *Biochemistry* 39:10219-10223.

Zanetti, G. and Forti, G. 1966. Studies on Triphosphopyridine Nucleotide-Cytochrome f Reductase of Chloroplasts. *J Biol Chem* 241(2):279-285.

Zhong, Q.; Inniss, D.; Kjoller, K. *et al*. 1993. Fractured polymer/silica fiber surface studied by tapping mode atomic force microscopy. *Surface Sci Lett* 290: 888-692.